

Document downloaded from:

<http://hdl.handle.net/10251/131994>

This paper must be cited as:

Romero-Peña, JS.; Cardona Marcet, N. (2010). Applicability Limits of Simplified Human Blockage Models at 5G mm-Wave Frequencies. IEEE. 1-5.
<http://hdl.handle.net/10251/131994>



The final publication is available at

<https://ieeexplore.ieee.org/document/8739476>

Copyright IEEE

Additional Information

Applicability Limits of Simplified Human Blockage Models at 5G mm-Wave Frequencies

J. Samuel Romero-Peña, Narcís Cardona
iTEAM Research Institute, Universitat Politècnica de València
Valencia, Spain
jhrope@iteam.upv.es

Abstract—This paper analyzes the feasibility of using a simple diffraction model to compute the blocking of the human body to millimeter wave radio frequencies in indoor environments. The model makes a set of approximations that are evaluated in the paper, to determine the applicability limits of such simplified approach to the human body blockage case. The work presented here: (1) describes briefly the mathematical support that is used to model the concealment using the Knife-Edge model, (2) identifies the potential simplifications applicable to the mathematical model implementation that allow a 3D geometric human body to be modelled with simple 2D shapes, (3) characterizes the polarization influence on the mm-wave blocking for such simplified human body models.

Keywords— *Millimeter-wave (mm-Wave), fifth-generation (5G), human blockage model, Knife-Edge diffraction*

I. INTRODUCTION

The current widespread use of the mobile technologies has created a huge demand for higher bandwidths, above those defined for previous generations of 3GPP networks based on LTE or UMTS. In the definition of the fifth generation (5G) standards this services demand is described as eMBB (Enhanced Mobile Broadband) and, among other technical approaches, the use of millimetre-wave frequencies (around and above 30GHz) has been proposed to allocate wideband mobile services [1][2].

The use of millimetre wave frequencies for mobile communications opens new challenges in the radio channel modelling, as almost all objects in indoor or outdoor environments are electrically large at millimetre-wave (mm-Wave) frequencies. In addition, the radio channel cannot be considered wide sense stationary at those frequencies, with effects caused by the transceivers movement and the multiple moving obstacles in the channel link, like humans (indoor-outdoor) and vehicles (outdoor), which change the characteristics of the channel in the very short term.

In our case study, we are considering the effect human body blockage in indoor environment millimetre wave propagation. In this scenario the human body is modelled as a non-static obstacle that is electrically large enough to generate temporary variations [3][4] of the channel as it moves within any environment. It is worth noting that the effect of human body blockage is integrated in the channel model as part of its dynamic behaviour, according to the body movement and morphology.

In our study, we determine the applicability of certain simplifications in the morphological model of the body, and so the potential reduction of the mathematical model complexity and computation time. A geometrically and electrically equivalent model for the human body is proposed and analysed. The final objective is to produce a simulation

tool as much realistic as possible that calculates temporal variations of the radio channel in real time. The key contributions of this paper are:

- Determination of the viability of using the simplified mathematical model of multiple knife-edge, which usefulness has already been validated in literature [7].
- Analyse a first approximation of the human body morphology as the combination of elliptical cylinders, for legs, arms and torso [7] [8].
- Consider the influence of polarization at these frequency bands in terms of the electrical dimensions of the human body, and its application to the proposed mathematical model [11].

II. HUMAN BLOCKAGE SIMPLIFIED MODELS

Our first approach to the human blockage model is based on obtaining the equivalent far field radiation path of an antenna when distorted by a blocking object that models the human body. Multiple knife-edge diffraction is calculated, tracing the dominant propagation paths in every scenario analyzed.

Double Knife-Edge (DKE) Model of an Absorbing Screen:

The human body has been extensively modelled as an absorbent screen due to the depth of penetration in millimetre waves. The simplest shape of such screen is a vertically-infinitesimal strip and it's called a double knife-edge (DKE) model as illustrated in figure .1 [5]

This model gives a reasonable approximation of the values of the far field at the receiver (Rx) when the human body is blocking the direct path, by calculating the double knife-edge diffraction from the absorbing screen. Initially, only the diffracted fields from the two sides of the absorbing screen are considered (Path-A, Path-B) [14]. According to [5] the DKE model [5] is applicable for $d_{Tx}, d_{Rx} \gg h$ and $d_{Tx}, d_{Rx} \gg \lambda$.

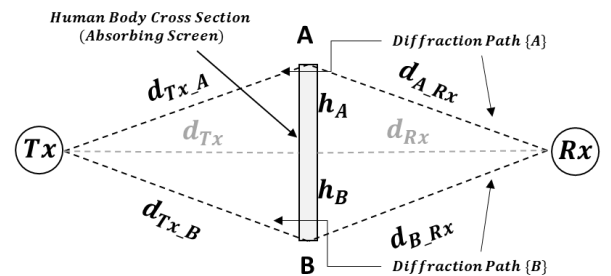


Figure 1 . Double Knife-Edge Model

The mathematical model (DKE) allows obtaining the normalized field diffracted at the Rx position, according the following expressions:

$$\frac{E}{E_0} = \left(\frac{1+j}{2}\right) \left[\left(\frac{1}{2} - C(v)\right) - j \left(\frac{1}{2} - S(v)\right) \right] \quad (1)$$

Where $C(v)$ and $S(v)$ are cosine and sine Fresnel integrals, and the parameter v is defined as the ratio between the different path lengths from the blocking element edges to the transmitter and receiver, and quantifies the diffraction concealment of the obstacle:

$$v = \pm h \sqrt{\frac{2}{\lambda}} \left(\frac{1}{d_{Tx}} + \frac{1}{d_{Rx}} \right) \quad (2)$$

where λ is the wavelength, d_{Tx} is the distance from the transmitter (Tx) to the blockage absorbing screen, d_{Rx} is the distance from the receiver (Rx) to the blockage absorbing screen, and h is the obstruction/shadow height produced by the obstacle (see h_a and h_b in figure 1). This v parameter indicates how the incident field is diffracted depending on the shadow generated by the absorbing screen, which directly depends on the Fresnel radius. The sign uncertainty of the parameter (v) depends on the visibility between T_x and R_x , and whether the obstacle is within the influence zone of the first Fresnel radius or not. Therefore in a LOS scenario there is a negative concealment $v(-)$, while for NLOS the concealment is positive $v(+)$.

As shown in Fig.1, the double knife-edge model calculates two diffraction paths independently, being the reference line-of-sight field given by:

$$E_0 = \frac{\lambda}{4\pi(d_{Tx}+d_{Rx})} e^{-j2\pi\frac{(d_{Tx}+d_{Rx})}{\lambda}} \quad (3)$$

Moreover, the total field at the receiver (Rx):

$$E_T = E_{2KE} = E_A e^{-j2\pi\left(\frac{\Delta d_A}{\lambda}\right)} + E_B e^{-j2\pi\left(\frac{\Delta d_B}{\lambda}\right)} \quad (4)$$

Where E_A and E_B are diffracted fields observed at the receiver (Rx) and Δd_A and Δd_B are given by:

$$\Delta d_A = (d_{Tx-A} + d_{A-Rx}) - (d_{Tx} + d_{Rx}) \quad (5)$$

$$\Delta d_B = (d_{Tx-B} + d_{B-Rx}) - (d_{Tx} + d_{Rx}) \quad (6)$$

The DKE diffraction model described above does not consider the polarization of the incident wave, because the human body is modelled as an absorbing infinitesimally thin screen. In section III of this paper the polarization influence is analyzed for the general case to obtain the minimum electrical dimensions of the modelled obstacle to assume that diffracted far field does not depend on polarization.

Another of the advantages of using this simple model is that it can be extended to characterize the multiple diffraction in indoor scenarios where there may surely be multiple people and obstacles shadowing the propagation paths [15][13]. For this reason, one of the main objectives of this paper is to characterize the diffraction for different orientations and positions of the antenna and the diffracting elements that in this case model the human body.

III. APPLICABILITY LIMITS OF HUMAN BLOCKAGE MODELS

Several models with different levels of complexity have been proposed in the literature to characterize the human body blocking at millimetre-wave frequencies, all of them giving similar results. The most recent references can be found at [8], where the authors performed a comparative analysis of the following models: conducting screen and wedge models (UTD) [9], circular cylinder model (GTD) [10], electromagnetic field solver (MoM) [13], numerical integration [14], measurement-based model [15] and the mm-Magic project model [16].

First, it will be indispensable to carry out a preliminary analysis of the minimum electrical dimensions for which the DKE model is valid. As mentioned in section II, the DKE mathematical model used in this work performs better for $L_p \gg \lambda$ and $W_p \gg \lambda$. Anyway, as the computational load of the simulations directly depends on the electrical dimensions of the absorbing screen, this paper intends to find the minimum values of L_p and W_p from which the computational model gives a valid approach to the human body blocking effect, when modelled as a simple geometrical form.

These dimensions are used to define a simple reference obstacle for simulations to be compared with the results and measurements of literature papers, i.e. to calibrate our simulator with other authors' results.

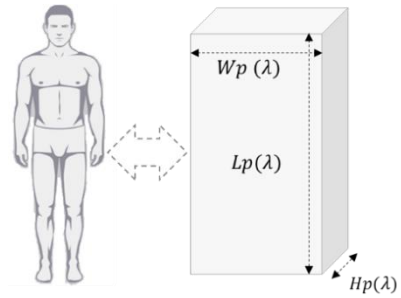


Figure 2. Human Body geometrical simplification.

Along the text, we refer to the equivalent geometry of the human body, according to every section context, with different forms such as cube, screen, cylinder or obstacle. Initially, we start considering the human body as a cube, as shown in figure 2. With this geometrical simplification we have three basic dimensions that are W_p (cube width), L_p (cube height) and H_p (cube thickness) *Note that according to our model $H_p \ll \lambda$ and W_p or L_p should be $\gg \lambda$.*

We analyze the influence of the electrical dimensions of the blocking element (W_p , L_p and H_p) by comparing the far field radiation pattern of the antenna with the equivalent far field radiation pattern when the obstacle is within the Tx-Rx path. In our simulations the blocking element is perpendicularly aligned (vertical) to the radiation pattern main axis of the antenna and the far field results analyzed over the horizontal plane.

In the coming subsections we describe the main results of an exhaustive analysis based on computer simulation (using CST tool) of the scenario described above, in order to define

the minimum electrical dimensions that W_p , L_p and H_p should have for the correct applicability of the DKE model. As deduced from these results, the dimensions of the human body, even if modelled separately by torso, head, arms and legs, are above the minimum dimensions that allow using a simple DKE for far field obstruction calculation.

(1) Distance [d_{Tx}] and Cube Width [W_p] Limits:

For the results shown in this section we analyzed the effect of the parameters d_{Tx} and W_p / L_p jointly. In figure 3, we have fixed the L_p dimension on the Y-Axis, and we vary progressively the W_p dimension on the X-Axis in order to observe significant differences over the far field on the Y-Axis.

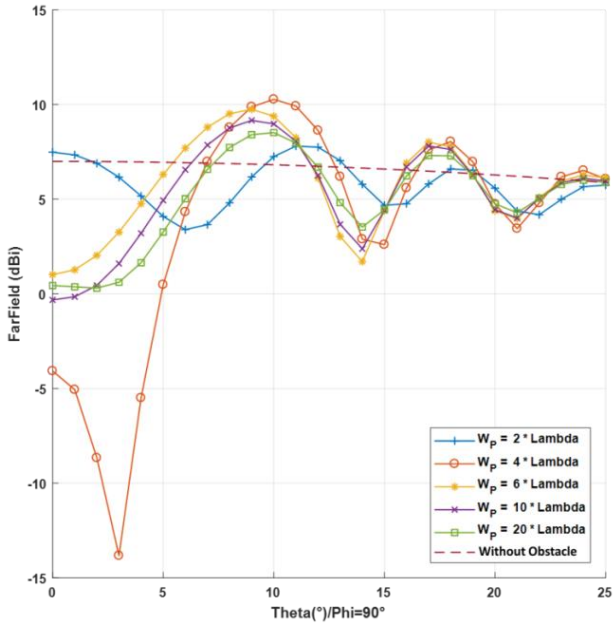


Figure 3. Equivalent far field radiation pattern (horizontal plane) in terms of blocking element width [W_p]

According to the results we can conclude that an infinitely wide/height screen ($L_p, W_p \gg \lambda$) can be simulated with dimensions above 10λ , since for higher widths no significant differences on the equivalent far field radiation pattern shape are observed (see figure 3).

As for the variation with the distance from the transmitter to the obstacle, the minimum distance from which the simplification to DKE is applicable depends on the electrical dimensions of the antenna and the dimensions of the blocking object. In our case, to obtain a reference value of this distance, we have used a standard patch antenna of 2 mm size designed in CST, and fixed the obstacle dimensions L_p and W_p to values above 10λ . The simulation results show that there are no significant variations of the far field shape from 15λ , but for any other antenna and obstacle sizes, the obtained minimum distance may differ.

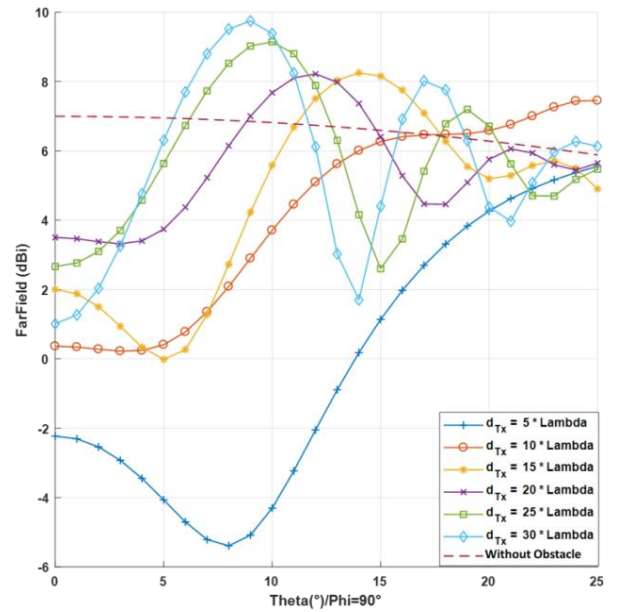


Figure 4. Equivalent far field radiation pattern (horizontal plane) in terms of the distance between blocking screen and Tx [d_{Tx}]

(2) Cube Thickness [H_p] Validation:

One of the main simplifications of the DKE model is that the absorbing screen is infinitesimally thin. In this section we analyze the influence of obstacle thickness on the far field computation results.

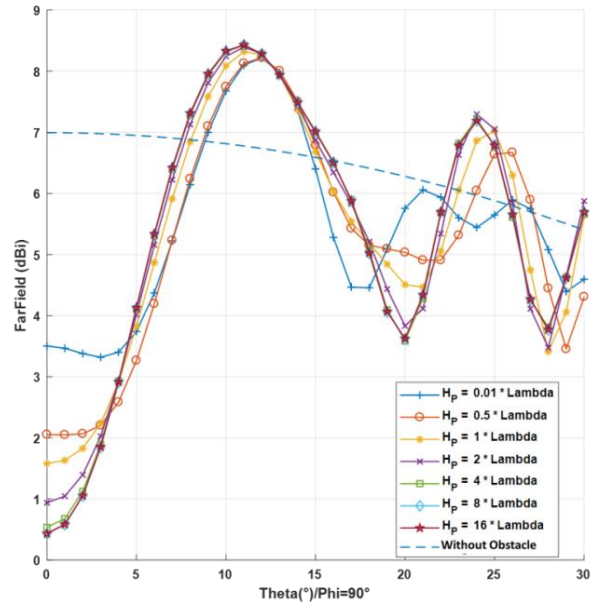


Figure 5. Equivalent far field radiation pattern (horizontal plane) vs blocking obstacle thickness (H_p)

Figure 5 shows the computation of the equivalent far field pattern for different thickness of the blocking element, when $L_p, W_p \gg \lambda$. According to the obtained results we can affirm that there are no significant variations in the shape of the diffracted far field when we use cubes of different thicknesses, so we can characterize the diffraction with an infinitesimally thin screen ($H_p \ll \lambda$).

(3) Geometrical Form Comparison

In some recent literature papers, the human body is modelled with a set of different elliptical cylinders of different dimensions [6]. In this section we determine the validity limits of the simplification of not considering the human body as a set of elliptical cylinders but as a set of infinitesimally thin screens ($H_p \ll \lambda$). For this reason we decided to make a comparative analysis of the diffracted far field generated by objects of several geometrical shapes, applying the electrical dimensions minimum limits for $W_p(\lambda), L_p(\lambda) > 10\lambda$, and varying the $H_p(\lambda)$ dimension of the cylinders.

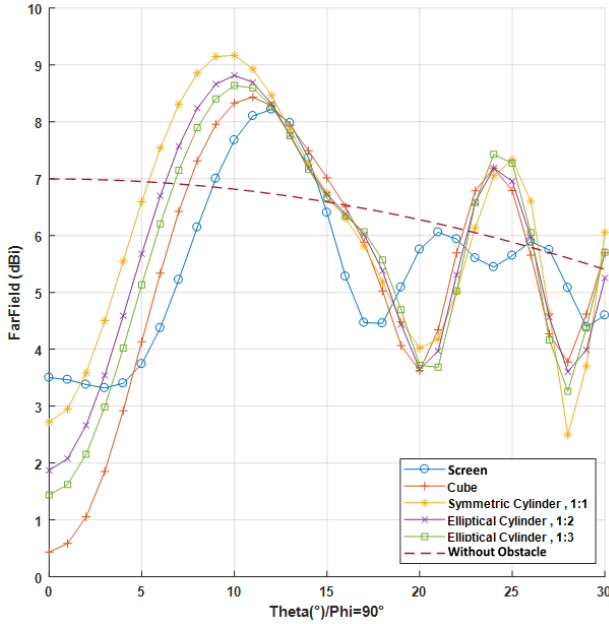


Figure 6. Equivalent far field radiation pattern (horizontal plane) for several shapes of the blocking (metallic) obstacle

Figure 6 shows the results for elliptical ratios of the cylinders from 1:1 to 1:3, being 1:3 the closest to the proportions of human body torso. In fact, the most used approximation in literature for the human body modelling at high frequencies is considering only the torso effect, as the main contribution to blocking. According to the obtained results, we can affirm that we can adequately model the shape behavior of the diffracted field of a symmetric or elliptical cylinder with an infinitesimally thin screen ($H_p \ll \lambda$).

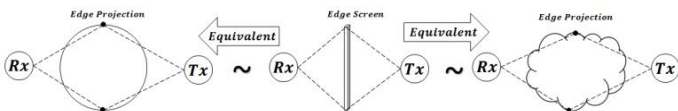


Figure 7. Equivalent diffracting edges to apply simple DKE to human body blockage model in computer simulations.

The application of our model to simulation of complex scenarios will use the above results, and will be based on calculating the DKE diffraction of the incident field only on

the visible edges of every obstacle (see figure 7), if the projected dimension of such obstacle on the incident field plane is larger than 10λ .

(4) Polarization Effect:

One of the major contributions of this paper was to identify the influence of the wave polarization on the geometric limits of the diffractive element, and how it affects, the validity of our model. Polarization effect has been usually neglected in many papers using simplified models for human blockage, but its influence is evident when measurements are reviewed [7]. To obtain the limiting dimensions, shapes and type of materials for which the polarization effect is significant, we have computed the diffracted far field after human body blocking using the previous sections model with the minimum electrical dimensions obtained.

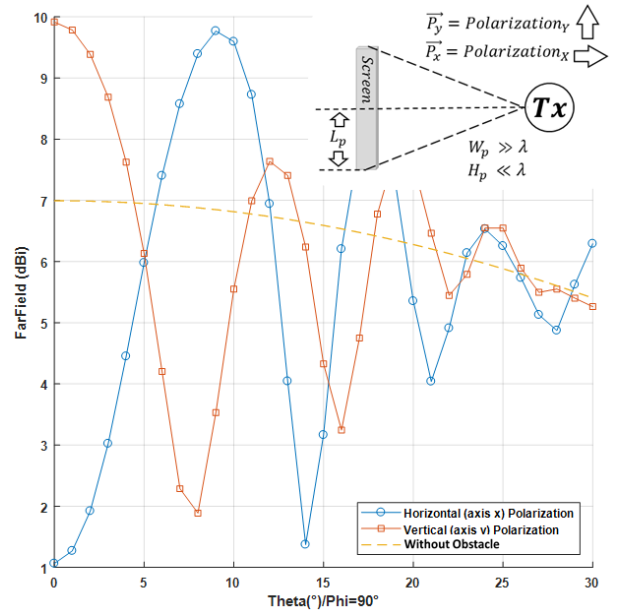


Figure 8. Equivalent far field radiation pattern (horizontal plane) for horizontal and vertical polarizations, $H_p \ll \lambda$ and $W_p \gg \lambda$

As shown in figure 8, when polarization of the incident wave is parallel to the diffracting edge (horizontal polarization), the blocking screen does not generate concealment over the far field, so the scattering on the incident field cannot be characterized with our simplified model directly. On the other hand, when polarization is perpendicular to the diffracting edge (vertical polarization), the concealment over the far field is as we have analyzed in previous sections and therefore the model is applicable.

According to the results shown in figure 9, we can conclude that the minimum electrical dimension L_p from which the polarization orientation does not influence the diffracted field is 10λ .

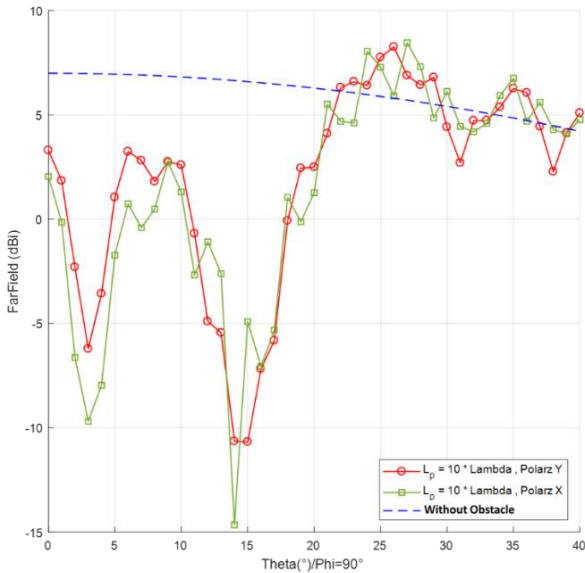


Figure 9. Results with two orthogonal polarizations on a thin screen with electrical dimensions: $W_p = 10 \lambda$, $L_p = 10 \lambda$, $H_p \ll \lambda$.

Our computer simulations also show that there is no influence of the polarization on the diffracted field for different shapes of the blocking element (Cube ($H_p > \lambda$) - Screen ($H_p \ll \lambda$) - Cylinder ($H_p > \lambda$)). Therefore we can model the effect of the human blocking with a thin screen of $H_p \ll \lambda$ despite of the polarization.

IV. CONCLUSIONS

In this paper we have determined the applicability limits of a simplified geometric model of the human body to calculate its blockage diffraction effect at mm-wave frequencies. Under these limits, the model proposed in [6] (Double Knife-Edge Model of an Absorbing Screen) can be assumed valid for such scenario. The obtained rules could be used to characterize other complex geometric forms of any diffracting object in built environments, not only of the human body.

The following basic rules to use DKE for human body modelling at mm-Wave frequencies are:

1. The minimum electrical dimension of the cross section of the blocking element shall be $W_p, L_p \geq 10\lambda$.
2. All geometrical shapes can be simplified to an absorbing screen infinitesimally thin $H_p \ll \lambda$.
3. The antenna polarization in the diffracted field only is relevant when $W_p, L_p < 10\lambda$.
4. The minimum distance from source to the absorbing screen model is 15λ , but will strongly depend on the antenna electrical size.

ACKNOWLEDGEMENTS

This work was supported by the H2020 Marie Curie program, with project grant no: 766231 WAVECOMBE-ITN-2017

REFERENCES

- [1] T. T. S. Rappaport, "Millimeter Wave Wireless Communications for 5G Cellular: It will work! Keynote presentation," pp. 335–349, 2014.
- [2] T. S. Rappaport, G. R. MacCartney, S. Sun, H. Yan, and S. Deng, "Small-Scale, Local Area, and Transitional Millimeter Wave Propagation for 5G Communications," *IEEE Trans. Antennas Propag.*, vol. 65, no. 12, pp. 6474–6490, 2017.
- [3] X. Chen, L. Tian, P. Tang, and J. Zhang, "Modelling of human body shadowing based on 28 GHz indoor measurement results," *IEEE Veh. Technol. Conf.*, no. 92, pp. 0–4, 2017.
- [4] G. R. Maccartney, T. S. Rappaport, and S. Rangan, "Rapid Fading Due to Human Blockage in Pedestrian Crowds at 5G Millimeter-Wave Frequencies," *2017 IEEE Glob. Commun. Conf. GLOBECOM 2017 - Proc.*, vol. 2018–Janua, pp. 1–7, 2018.
- [5] J. Kunisch and J. Pamp, "Ultra-wideband double vertical knife-edge model for obstruction of a ray by a person," *Proceedings 2008 IEEE Int. Conf. Ultra-Wideband, ICUWB 2008*, vol. 2, no. 2, pp. 17–20, 2008.
- [6] U. T. Virk and K. Haneda, "Modeling Human Blockage at 5G Millimeter-Wave Frequencies," 2018.
- [7] N. Tran, T. Imai, and Y. Okumura, "Study on Characteristics of Human Body Shadowing in High Frequency Bands," 2014.
- [8] C. Gustafson and F. Tufvesson, "Characterization of 60 GHz shadowing by human bodies and simple phantoms," *Radioengineering*, vol. 21, no. 4, pp. 979–984, 2012.
- [9] M. Yokota, T. Ikegama, Y. Ohta, and T. Fujii, "Numerical examination of EM wave shadowing by human body," *Antennas Propag. (EuCAP), 2010 Proc. Fourth Eur. Conf.*, pp. 4–7, 2010.
- [10] A. G. Aguilar, P. H. Pathak, and M. Sierra-Pérez, "A canonical UTD solution for electromagnetic scattering by an electrically large impedance circular cylinder illuminated by an obliquely incident plane wave," *IEEE Trans. Antennas Propag.*, vol. 61, no. 10, pp. 5144–5154, 2013.
- [11] P. Karadimas, B. Allen, and P. Smith, "Human body shadowing characterization for 60-GHz indoor short-range wireless links," *IEEE Antennas Wirel. Propag. Lett.*, vol. 12, pp. 1650–1653, 2013.
- [12] D. Number, P. Name, M. B. Mobile, R. Access, F. Generation, and I. Communications, "Measurement Results and Final mmMAGIC Channel Models Measurement Results and Final mmMAGIC Channel Models," 2017.